Title
Selective removal of dental calculus with a diode-pumped Er:YAG laser

Authors
Fried, William A
Chan, Kenneth H
Darling, Cynthia L
et al.

Publication Date
2019-02-01

DOI
10.1117/12.2512937

Peer reviewed

HHS Public Access

Author manuscript

Proc SPIE Int Soc Opt Eng. Author manuscript; available in PMC 2019 April 16.

Published in final edited form as:

Proc SPIE Int Soc Opt Eng. 2019 February ; 10857: . doi:10.1117/12.2512937.

Selective removal of dental calculus with a diode-pumped Er:YAG laser

William A. Fried, **Kenneth H. Chan**, **Cynthia L. Darling**, and **Daniel Fried**[•]

University of California, San Francisco, San Francisco, CA 94143-0758

Abstract

Selective removal of dental calculus with high precision is best accomplished using lasers operating at high pulse repetition rates focused to a small spot size to limit damage to sound tissues. Conventional flash-lamp pumped Er:YAG lasers are poorly suited for this purpose, but new diode-pumped solid state (DPSS) Er:YAG lasers have become available operating at high pulse repetition rates. The purpose of this study was to determine if image-guided laser ablation can be used to selectively remove calculus from tooth surfaces with minimal damage to the underlying sound cementum and dentin. A DPSS Er:YAG laser system was used to selectively remove calculus from ten extracted teeth using sequential SWIR images at 1500–1750-nm. The selectivity of removal was assessed using digital microscopy and optical coherence tomography. Calculus was removed with minimal damage to the underlying sound cementum and dentin.

Keywords

Er:YAG laser; dental calculus; SWIR imaging; image-guided laser ablation

1. INTRODUCTION

Calculus is formed sub- and supragingival and it contributes to irritation and inflammation of the gingiva leading to gingivitis and periodontitis. Scaling and root planing are typically employed to remove the calculus. A laser system that can rapidly and selectively remove calculus from tooth surfaces while minimizing the inadvertent removal of healthy tooth structure would be a significant improvement over current methods. Several studies report the use of lasers for the removal of calculus including the Er:YAG laser [1–6]. DPSS Er:YAG lasers with high pulse repetition rates are more suitable for the selective removal of dental caries, composites and calculus than existing Er:YAG lasers [7]. The flash-lamp pumped erbium solid-state lasers presently being used for dental hard tissue ablation are poorly suited for this approach since they utilize high energy pulses and relatively low pulse repetition rates. DPSS Er:YAG lasers are now available operating with pulse repetition rates as high as 1–2 kHz and initial studies have been carried out demonstrating their utility for the ablation of dental hard tissues and bone [8–10] and composite from tooth surfaces [11]. Previous approaches for guiding laser ablation on tooth surfaces have included fluorescence [12–14] and near-IR transillumination [15]. In addition to investigating the selective removal

[•]Contact Author: daniel.fried@ucsf.edu.

of caries lesions with a fluorescence based feedback system, Krause et al. [16] have investigated the removal of calculus.

Multiple studies both *in vitro* and *in vivo* on the coronal surfaces of teeth have demonstrated that short wavelength infrared (SWIR) reflectance imaging yields higher contrast between demineralized and sound tooth structure than visible reflectance and fluorescence. Much of this difference is because the stains do not interfere at wavelengths longer than 1200-nm [17–22]. SWIR wavelengths appears to be equally advantageous for imaging root caries and calculus due to the lack of interference of stains beyond 1200-nm and increased suppression of the reflectivity from the sound dentin due to higher water absorption which increases markedly beyond 1400-nm [23].

Image-guided laser ablation requires the rapid acquisition of high-contrast images of caries lesions or calculus that can be input into the laser-scanning system for selective removal. Computer control is now feasible due to the recent advances in compact high-speed laser scanning technology such as MEMS (Micro-Electro-Mechanical Systems) mirrors and miniature galvanometer “galvo” based scanners. One approach is to remove the lesion or calculus layer by layer, i.e. image the lesion then scan the laser and remove an outer layer of the lesion, then re-image and scan again repeating that process until the lesion is completely removed. Previous studies have demonstrated the feasibility of removing lesions by sequentially imaging carious teeth with an SWIR InGaAs camera or coaxial SWIR laser as the CO_2 laser removes the lesion layer by layer [24–26].

The purpose of this study was to explore the potential of using SWIR reflectance imaging with a DPSS Er:YAG laser for the image guided ablation of dental calculus.

2. MATERIALS AND METHODS

2.1 Sample Preparation

Ten teeth with prominent calculus deposits extracted from patients in the San Francisco Bay Area were collected, cleaned and sterilized with Gamma radiation and stored in a 0.1 % Thymol solution. Calculus was easily identified as dark gray or black clumps stuck to the tooth surface below the CEJ. Since calculus deposits protrude above the tooth cementum, calculus presence was confirmed using OCT. Teeth were mounted on 1 × 1 × 3 cm cylindrical blocks of black orthodontic composite resin with the root surface containing the lesions facing out from the square surface of the block. Each rectangular block fits precisely in an optomechanical assembly that could be positioned with micron accuracy. The samples were stored in a moist environment and they were air-dried with compressed air for ten seconds before measurement.

2.2 Visible and SWIR Cross Polarization Reflectance Images (SWIR)

Visible color images of the samples were acquired using a USB microscope, Model AM7915MZT from AnMO Electronics Corp. (New Taipei City, Taiwan) with extended depth of field and cross polarization. The digital microscope captures 5 mega-pixel (2,952 × 1,944) color images.

In order to acquire reflected light images, linearly polarized and collimated light from a 150-W fiber-optic illuminator, Model FOI-150 from the E. Light Company (Denver, Colorado) was used to illuminate the samples at an incident angle of 30° relative to the surface normal of the tooth root surface. Polarizers were placed after the light source and before the detector to remove specular reflection (glare) that interferes with measurements of the lesion contrast. The SWIR reflectance images were captured using a 12-bit Model GA1280J (Sensors Unlimited, Princeton, NK) with a 1280 × 1024 pixel format and 15-μm pixel pitch with ISR-P lens. Reflectance measurements were taken with a 1500-nm long-pass filter, FEL 1500 from Thorlabs (Newton, NJ) over the range of 1500–1750-nm.

2.3 Laser Setup and Parameters

Samples were irradiated using a DPSS Er:YAG laser, Model DPM-30 from Pantec Engineering, (Liechtenstein) operated at a pulse duration of 50-μs and a pulse repetition rate of 50-Hz. The laser energy output was monitored using a power meter EPM 1000, Coherent-Molectron (Santa Clara, CA), and the Joulemeter ED-200 from Gentec (Quebec, Canada). A high-speed XY-scanning system, Model ESP 301 controller with ILS100PP and VP-25AA stages from Newport (Irvine, CA) was used to scan the samples across the laser beam. The laser was focused to a spot size of ~330-μm using an ZnSe lens of 75 mm focal length. A pressure air-actuated fluid spray delivery system consisting of a 780S spray valve, a Valvemate 7040 controller, and a fluid reservoir from EFD, Inc. (East Providence, RI) were used to provide a uniform and continuous spray of fine water mist onto the tooth surfaces at 2 mL/min. An incident fluence of 9 J/cm^2 was used to remove the calculus from tooth surfaces.

2.4 Digital Microscopy

Tooth surfaces were examined after laser irradiation using an optical microscopy/3D surface profilometry system, the VHX-1000 from Keyence (Elmwood, NJ). Two lenses were used, the VH-Z25 with a magnification from 25 to 175× and the VH-Z100R with a magnification of 100–1000×. Depth composition digital microscopy (DCDM) images and 3D images were acquired by scanning the image plane of the microscope and reconstructing a depth composition image with all points at optimum focus displayed in a 2D image. The Keyence 3-D measurement software, VHX-H3M, was used to examine the laser-irradiated surfaces for residual calculus and damage to the underlying cementum and dentin.

2.5 Imaging, Processing, and Calculus Removal

Samples were air-dried for ~20 seconds prior to acquisition of SWIR images of the occlusal surface of each tooth. To obtain accurate backscattered light intensity values in SWIR reflectance images from a non-uniform illumination source, SWIR reflectance images are calibrated with a background reference. Contrast maps were constructed by subtracting the background reference. Intensity values from the initial scan were collected and reused throughout the caries removal process to maintain repeatability in lesion segmentation. The mean intensity of sound enamel I_S is calculated over a region of sound enamel and the maximum intensity of the demineralization I_D is collected inside the lesion area. The pixel contrast C is computed by subtracting the intensity of the image pixel I_P with the mean intensity of sound enamel and the minimum value I_{MIN} in each image and dividing this difference over the maximum intensity. An image ablation map or look-up table (LUT) is generated by comparing the pixel contrast to a specified threshold over the enhanced SWIR image.

$$\text{If } C = \left(I_P\text{-}I_{MIN}\text{-}I_S\right)/I_D > T\text{; add pixel to LUT}$$

Samples were mounted on a separate system for Er:YAG laser ablation, and positioned precisely to match the orientation as the one used for SWIR imaging. Repeated serial SWIR images were acquired to update the LUT's and the ablation scans were repeated until all the calculus was removed. All image analysis was carried out using Labview (National Instruments) and Igor pro software (Wavemetrics, Lake Oswego, OR).

2.6 Optical Coherence Tomography (OCT)

An autocorrelator-based Optical Coherence Domain Reflectometry (OCDR) system with an integrated fiber probe, high efficiency piezoelectric fiber-stretchers and two balanced InGaAs receivers that was designed and fabricated by Optiphase, Inc. (Van Nuys, CA) was integrated with a broadband high power superluminescent diode (SLD), DL-CS313159A from Denselight (Jessup, MD) operating at 1304-nm with an output power of 19-mW and a bandwidth of 83 nm and a high-speed XY-scanning system, ESP 300 controller & 850-HS stages from Newport (Irvine, CA) and used for *in vitro* optical tomography. The fiber probe was configured to provide an axial resolution at 9-µm in air and 6-µm in enamel and a lateral resolution of approximately 50-µm over the depth of focus of 10-mm.

The all-fiber OCDR system has been previously described in greater detail [27]. The OCT system is completely controlled using Labview™ software from National Instruments (Austin, TX). Acquired scans are compiled into *b-scan* files. Image processing was carried out using Igor Pro™, data analysis software from Wavemetrics Inc, (Lake Oswego, Oregon). The processed images were then analyzed using Avizo software (ThermoFisher, Hillsboro, OR).

3. RESULTS AND DISCUSSION

There was nearly complete removal of all calculus within the treatment area for all of the samples. Half the samples had small localized of residual calculus deposits similar to those visible for the sample shown in Fig. 1. It is possible that these residual deposits of calculus have hardened from the repeated scans from the laser, making them more resistant to further attempts to remove them. The sample shown in Fig. 1 is one of the samples that had the largest number of residual deposits of calculus after the removal process was completed. Figure 1 contains the color images of the tooth before and after removal along with SWIR images at 1500–1750-nm, OCT images and high-resolution images taken using digital microscopy. There are some stained areas remaining after removal visible in the color images and these areas are not visible in the SWIR images. Most likely, these deposits are either non-calcified plaque or some other organic material that has attached itself to the tooth surface. There was minimal damage to the underlying cementum/dentin layer on the sample shown in Fig. 1. However, for half of the samples there were localized areas of substantial removal of cementum/dentin. Those areas were typically close to the cementum-enamel junction which suggests that they may be areas of demineralization due to root caries lying under the calculus. Since subsurface demineralization appears similar to calculus at SWIR wavelengths, those areas are selectively removed in addition to the overlying calculus. In summary, this pilot study suggests that SWIR image-guided laser ablation of dental calculus is promising using the DPSS Er:YAG laser.

ACKNOWLEDGMENTS

This work was supported by NIH/NIDCR Grant R01-DE19631.

5. REFERENCES

[1]. Aoki A, Ando Y, Watanabe H, and Ishikawa I, “In vitro studies on laser scaling of subgingival calculus with an erbium:YAG laser,” J Periodontol, 65(12), 1097–106 (1994). [PubMed: 7877081]

[2]. Aoki A, Miura M, Akiyama F, Nakagawa N, Tanaka J, Oda S, Watanabe H, and Ishikawa I, “In vitro evaluation of Er:YAG laser scaling of subgingival calculus in comparison with ultrasonic scaling,” J Periodontal Res, 35(5), 266–77 (2000). [PubMed: 11005154]

[3]. Radvar M, Creanor SL, Gilmour WH, Payne AP, McGadey J, Foye RH, Whitters CJ, and Kinane DF, “An evaluation of the effects of an Nd:YAG laser on subgingival calculus, dentine and cementum. An in vitro study,” J Clin Periodontol, 22(1), 71–7 (1995). [PubMed: 7706542]

[4]. Rechmann P, “Dental laser research: selective ablation of caries, calculus, and microbial plaque: from the idea to the first in vivo investigation,” Dent Clin North Am, 48(4), 1077–104 (2004). [PubMed: 15464565]

[5]. Ting CC, Fukuda M, Watanabe T, Aoki T, Sanaoka A, and Noguchi T, “Effects of Er,Cr:YSGG laser irradiation on the root surface: morphologic analysis and efficiency of calculus removal,” J Periodontol, 78(11), 2156–64 (2007). [PubMed: 17970683]

[6]. Tucker D, Cobb CM, Rapley JW, and Killoy WJ, “Morphologic changes following in vitro CO2 laser treatment of calculus-ladened root surfaces,” Lasers Surg Med, 18(2), 150–6 (1996). [PubMed: 8833283]

[7]. Yan R, Chan KH, Tom H, Simon JC, Darling CL, and Fried D, “Selective removal of dental caries with a diode-pumped Er:YAG laser,” Lasers in Dentistry XX. Proc SPIE Vol. 9306 (O)1–8 (2015).

[8]. Stock K, Diebolder R, Hausladen F, and Hibst R, “Efficient bone cutting with the novel diode pumped Er:YAG laser system: in vitro investigation and optimization of the treatment parameters,” Lasers in Dentistry XVIII, Proc SPIE Vol. 8926, (P) 1–6 (2014).

[9]. Stock K, Diebolder R, Hausladen F, Wurm H, Lorenz S, and Hibst R, “Primary investigations on the potential of a novel diode pumped Er:YAG laser system for bone surgery,” Photonic Therapeutics and Diagnostics IX, Proc SPIE Vol. 8565, (D) 1–8 (2013).

[10]. Stock K, Hausladen F, and Hibst R, “Investigations on the potential of a novel diode pumped Er:YAG laser system for dental applications,” Lasers in Dentistry XVI, Proc SPIE Vol. 8208, (D)1–5 (2012).

[11]. Fried WA, Chan KH, Darling CL, and Fried D, “Use of a DPSS Er:YAG laser for the selective removal of composite from tooth surfaces,” Biomed Opt Express, 9(10), 5026–5036 (2016).

[12]. Eberhard J, Bode K, Hedderich J, and Jepsen S, “Cavity size difference after caries removal by a fluorescence-controlled Er:YAG laser and by conventional bur treatment,” Clinical oral investigations, 12(4), 311–8 (2008). [PubMed: 18500542]

[13]. Eberhard J, Eisenbeiss AK, Braun A, Hedderich J, and Jepsen S, “Evaluation of selective caries removal by a fluorescence feedback-controlled Er:YAG laser in vitro,” Caries Res, 39(6), 496–504 (2005). [PubMed: 16251795]

[14]. Jepsen S, Acil Y, Peschel T, Kargas K, and Eberhard J, “Biochemical and morphological analysis of dentin following selective caries removal with a fluorescence-controlled Er:YAG laser,” Lasers Surg Med, 40(5), 350–7 (2008). [PubMed: 18563782]

[15]. Tao YC, and Fried D, “Near-infrared image-guided laser ablation of dental decay,” J Biomed Optics, 14(5), 054045 (2009).

[16]. Krause F, Braun A, Brede O, Eberhard J, Frentzen M, and Jepsen S, “Evaluation of selective calculus removal by a fluorescence feedback-controlled Er:YAG laser in vitro,” J Clin Periodontol, 34(1), 66–71 (2007). [PubMed: 17132156]

[17]. Jones RS, Huynh GD, Jones GC, and Fried D, “Near-IR Transillumination at 1310-nm for the Imaging of Early Dental Caries,” Optics Express, 11(18), 2259–2265 (2003). [PubMed: 19466117]

[18]. Buhler C, Ngaotheppitak P, and Fried D, “Imaging of occlusal dental caries (decay) with near-IR light at 1310-nm,” Optics Express, 13(2), 573–82 (2005). [PubMed: 19488387]

[19]. Staninec M, Lee C, Darling CL, and Fried D, “In vivo near-IR imaging of approximal dental decay at 1,310 nm,” Lasers Surg Med, 42(4), 292–8 (2010). [PubMed: 20432277]

[20]. Chung S, Fried D, Staninec M, and Darling CL, “Multispectral near-IR reflectance and transillumination imaging of teeth “ Biomed Opt Express, 2(10), 2804–2814 (2011). [PubMed: 22025986]

[21]. Fried WA, Chan KH, Fried D, and Darling CL, “High Contrast Reflectance Imaging of Simulated Lesions on Tooth Occlusal Surfaces at Near-IR Wavelengths,” Lasers Surg Med, 45(8), 533–541 (2013). [PubMed: 23857066]

[22]. Simon JC, Lucas SA, Lee RC, Staninec M, Tom H, Chan KH, Darling CL, and Fried D, “Near-IR Transillumination and Reflectance Imaging at 1300-nm and 1500–1700-nm for in vivo Caries Detection,” Lasers Surg Med, 48(6), 828–836 (2016). [PubMed: 27389018]

[23]. Yang VB, Curtis DA, Fried D, and “Cross-polarization reflectance imaging of root caries and dental calculus at wavelengths from 400–2350-nm,” J Biophotonics, 11, e201800113 (2018). [PubMed: 29952066]

[24]. Chan KH, Tom H, Darling CL, and Fried D, “Serial removal of caries lesions from tooth occlusal surfaces using near-IR image-guided IR laser ablation,” Lasers in Dentistry XIX, Proc SPIE Vol. 9306, (G) 1–6 (2015).

[25]. Chan KH, and Fried D, “Selective ablation of dental caries using coaxial CO2 (9.3-μm) and near-IR (1880-nm) lasers,” Lasers Surg Med, doi: 10.1002/lsm.23002. [Epub ahead of print] (2019).

[26]. Tom H, Chan KH, Darling CL, Pelzner R, and Fried D, “Selective removal of demineralized enamel using a CO_2 laser coupled with near-IR reflectance imaging,” Lasers Surg Med, 48(1), 52–61 (2016). [PubMed: 26763111]

[27]. Bush J, Feldchtein F, Gelikonov G, Gelikonov V, and Piyevsky S, “Cost effective all-fiber autocorrelator for optical coherence tomography imaging,” 17th International Conference on Optical Fibre Sensors, Proc. SPIE Vol. 5855, 254–7 (2005).

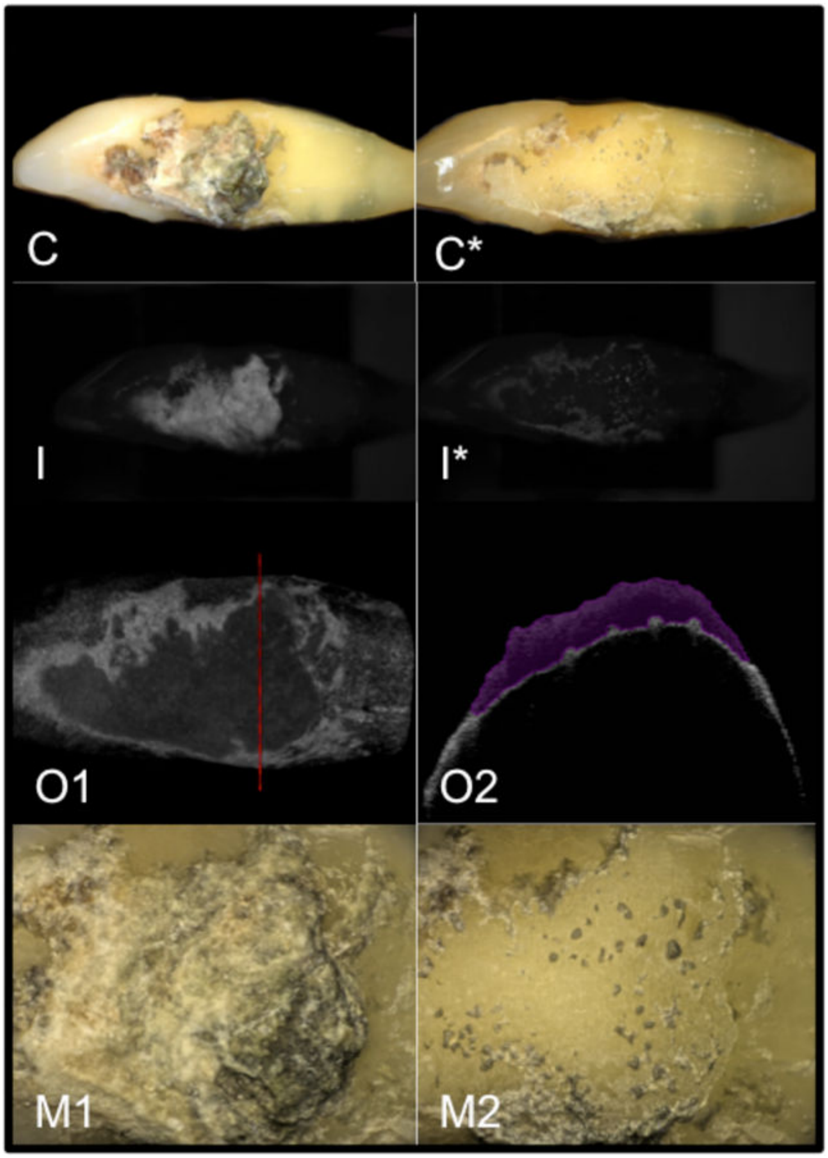

Fig. 1.

Color images (C & C*) and NIR (I & I*) before and after calculus removal. (O1) A surface rendering of the 3D OCT image is shown with the position of the extracted b-scan (O2) indicated by the red line. Overlays of co-registered OCT scans were used to determine the calculus removed shown in purple. Digital microscope images taken at 50 magnification show the laser irradiated area pre (M) and post-treatment (M*).